 Proceedings of ICCES'08, pp.779-784

Numerical Investigation on Resonant Sloshing Characteristics of 2-D Baffled Liquid Container

Jong-Kook Cha[1] and Jin-Rae Cho[1]

Summary

Sloshing flow is formulated based on the linearized potential flow theory, while an artificial damping term is employed into the kinematic free-surface condition to reflect the eminent dissipation effect in resonant sloshing. Through the numerical analysis of sloshing frequency response with respect to the number, location and opening width of baffle, the sloshing damping characteristics by baffle are parametrically investigated.

Introduction

In the resonant sloshing analysis, the damping effect should not be ignored in order to prevent the divergence in the frequency response near resonance frequencies. However, differing from the numerical sloshing analysis in time domain [1], a consideration of full viscous flow for the case in frequency domain leads to complicated large-scale matrix equations in the form of complex variable. In order to reflect the damping effect while assuming inviscid liquid flow, Faltinsen [2] proposed an artificial dissipation mechanism based on the Rayleigh damping concept. A product of the artificial viscosity coefficient and the velocity potential gradient is added into the Euler equation, from which the kinematic free-surface condition with the artificial damping term is derived through a modified Bernoulli equation. Where, the artificial viscosity coefficient is defined by the relative damping ratio to the critical damping.

This paper investigates the resonance frequency response of liquid sloshing in baffled 2-D tank by a finite element method. While employing the kinematic free-surface condition with the artificial damping term, we formulate the resonance frequency response according to the linearized potential flow theory. The reliability of the numerical solutions is assessed by the comparison with the analytical solutions [2]. The effects of baffle on the resonance sloshing response are investigated with respect to the major baffle parameters.

Sloshing Flow in 2-D Rigid Baffled Container

Fig. 1 shows a two-dimensional rectangular tank with a pair of baffles in which interior liquid is filled up to the height H_L from the tank bottom in the stationary condition. Both tank and baffle are assumed to be rigid, and the horizontal harmonic excitation is applied to the whole tank. A Cartesian co-ordinate system is originated at the center of the undisturbed free surface. Even though the baffle thickness is

[1]School of Mechanical Engineering, Pusan National University, Busan 609-735, Korea

neglected, the boundary of the liquid domain Ω is composed of the liquid-structure interface $\partial\Omega_I$ and the free surface $\partial\Omega_F$.

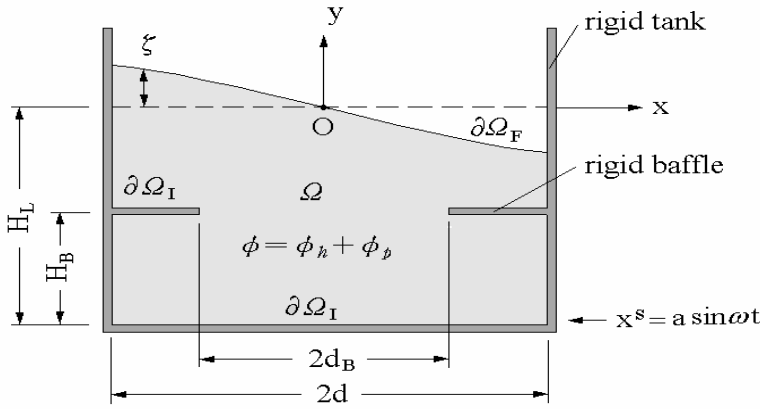

Figure 1: Liquid sloshing in 2-D baffled tank by horizontal harmonic excitation.

We assume the liquid is inviscid incompressible and the sloshing flow irrotational so that there exists a velocity potential function ϕ satisfying

$$\nabla^2\phi = 0, \quad \text{in } \Omega \tag{1}$$

with the structure-liquid interface condition: $\nabla\phi\cdot\mathbf{n} = \mathbf{u}^s\cdot\mathbf{n}$ on $\partial\Omega_I$. Here, $\mathbf{n}$ denotes the outward unit vector normal to the liquid boundary and $\mathbf{u}^s = \{a\omega\cos\omega t, 0\}$ is the tank velocity. To the free surface, we specify the linearized dynamic and kinematic conditions given by

$$\frac{\partial\phi}{\partial t} + g\zeta + \mu\phi = 0, \quad \text{on } \partial\Omega_F, \quad \frac{\partial\phi}{\partial y} = \frac{\partial\zeta}{\partial t}, \quad \text{on } \partial\Omega_F \tag{2}$$

where ζ is the elevation of liquid free surface. Meanwhile, the term $\mu\phi$ is the nothing but the artificial damping introduced to prevent the divergence phenomenon at resonance frequencies. Taking the time derivative to Eq. (2) leads to a unified free-surface condition given by

$$\frac{\partial^2\phi}{\partial t^2} + g\frac{\partial\phi}{\partial y} + \mu\frac{\partial\phi}{\partial t} = 0, \quad \text{on } \partial\Omega_F \tag{3}$$

The hydrodynamic pressure p and the free-surface elevation ζ in the linearized sloshing flow with the artificial surface damping are calculated as

$$p = -\rho\left(\frac{\partial\phi}{\partial t} + \mu\phi\right), \quad \text{in } \Omega, \quad \zeta = -\frac{1}{g}\left(\frac{\partial\phi}{\partial t} + \mu\phi\right), \quad \text{on } \partial\Omega_F \tag{4}$$

Finite Element Approximation in Frequency Domain

Applying the virtual work principle to Eq. (1), together with the boundary conditions, leads to the following variational formulation:

$$\int_{\Omega} \nabla\phi \cdot \nabla\psi \, d\Omega = -\frac{1}{g}\int_{\partial\Omega_F} \frac{\partial^2\phi}{\partial t^2}\,\psi\, ds - \frac{\mu}{g}\int_{\partial\Omega_F} \frac{\partial\phi}{\partial t}\,\psi\, ds + a\omega\cos\omega t \int_{\partial\Omega_I^R} \psi\, ds - a\omega\cos\omega t \int_{\partial\Omega_I^L} \psi\, ds \tag{5}$$

Here, $\partial\Omega_I^R$ denotes the right side wall and $\partial\Omega_I^L$ the left side wall of the tank, respectively. We let ϕ be in function of cosine with the phase angle β and use 9-node iso-parametric basis functions $\{N_i\}_{i=1}^N$ to expand trial and test functions

$$\phi = \sum_{i=1}^{N} N_i\,\bar{\phi}_i \cos(\omega t - \beta), \quad \psi = \sum_{i=1}^{N} N_i\,\bar{\psi}_i \cos(\omega t - \beta) \tag{6}$$

Then, the previous variational formulation leads to the matrix equations given by

$$\left[K - \omega^2 M\right]\,\bar{\phi}\cos(\omega t - \beta) - \omega C\,\bar{\phi}\sin(\omega t - \beta) = \omega F\cos\omega t \tag{7}$$

where $\bar{\phi}$ is defined by the vector of nodal velocity potentials. The matrices in Eq. (7) are defined respectively by ($C = \mu M$)

$$K = \int_{\Omega} (\nabla N)^T (\nabla N)\, d\Omega, \quad M = \frac{1}{g}\int_{\partial\Omega_F} N^T N\, ds \tag{8}$$

$$F = a\int_{\partial\Omega_I^R} N^T\, ds - a\int_{\partial\Omega_I^L} N^T\, ds \tag{9}$$

In order to establish the modal equations of Eq. (7), we first compute the natural sloshing frequencies and modes with

$$\left[K - \omega^2 M\right]\,\bar{\phi} = 0 \tag{10}$$

Realizing that the mass matrix M is restricted to only the finite element nodes of the liquid free surface $\partial\Omega_F$, Eq. (10) can be decomposed as follows [3]:

$$\begin{bmatrix} K_{SS} & K_{SI} \\ K_{IS} & K_{II} \end{bmatrix} \begin{Bmatrix} \bar{\phi}_S \\ \bar{\phi}_I \end{Bmatrix} - \omega^2 \begin{bmatrix} M & 0 \\ 0 & 0 \end{bmatrix} \begin{Bmatrix} \bar{\phi}_S \\ \bar{\phi}_I \end{Bmatrix} = \begin{Bmatrix} 0 \\ 0 \end{Bmatrix} \tag{11}$$

Subscripts S and I are used to stand for the free surface nodes and the remaining interior liquid nodes, respectively.

According to the static condensation we obtain the reduced eigen matrix equations for the free surface sloshing given by

$$\left[K_{SS} - K_{SI}K_{II}^{-1}K_{IS}\right]\bar{\phi}_S - \omega^2 M\bar{\phi}_{\mathbf{S}} = 0, \quad \bar{\phi}_I = -K_{II}^{-1}K_{IS}\bar{\phi}_S \tag{12}$$

Next, we expand the nodal potential vector $\bar{\phi}$ in terms of only the sine modes among N_S natural modes such that

$$\bar{\phi}(\mathbf{x};\omega) = \sum_{i=1}^{N_S^*} \bar{\phi}_n^i(\mathbf{x}) \cdot q_i(\omega) \tag{13}$$

where q_i are defined as the modal participation coefficients to be determined. Letting $Q_k = \left(\bar{\phi}_n^k\right)^T F$ and plugging Eq. (13) into Eq. (7) and premultiplying the resulting equation by $\left(\bar{\phi}_n^k\right)^T$ lead to N_S^* uncoupled modal equations for $\{q_k\}$:

$$\left[\left(\omega_n^k\right)^2 - \omega^2\right] q_k \cos(\omega t - \beta) - \omega\mu\, q_k \sin(\omega t - \beta) = \omega\, Q_k \cos\omega t \tag{14}$$

Applying the basic relation of triangular functions to Eq. (14), one can derive the angles and participation coefficients are determined according to

$$\beta_k = \tan^{-1}\left(\frac{\mu\omega}{\left(\omega_n^k\right)^2 - \omega^2}\right), \quad q_k = \pm\omega\, Q_k \cdot \left[\left(\left(\omega_n^k\right)^2 - \omega^2\right)^2 + (\mu\omega)^2\right]^{-1/2} \tag{15}$$

where q_k is positive when $\omega_n > \omega$ and vice versa. Then, we finally have the finite element approximation of the total velocity potential given by

$$\phi = \sum_{i=1}^{N} N_i \left(\sum_{k=1}^{N_S^*} q_k \bar{\phi}_n^k \cos(\omega t - \beta_k)\right)_i \tag{16}$$

Numerical Experiment

We consider a baffled container under the horizontal harmonic excitation $x^S = a\sin\omega t$, in which the number, the installation height and the opening width of baffle are taken variable. Geometry, material and excitation data are recorded in Table 1, where the excitation frequency ω taken as an input variable is varying with the increment $\Delta\omega$ of $0.001\,rad/s$. The liquid domain Ω is uniformly discretized with 9-node quadratic elements such that the total element number is 300. Referring to Fig. 2, baffles are installed with uniform vertical spacing and the occurrence of zero-thicknessed baffle is numerically implemented by separating liquid nodes.

The effect of the baffle number on the frequency response of free-surface elevation near the fundamental resonance frequency is presented in Fig. 3. The relative

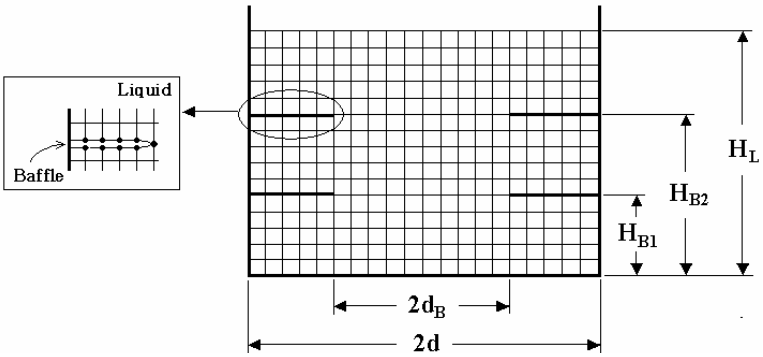

Figure 2: Finite element mesh of a baffled container.

Table 1: Simulation data taken for the verification experiments

Liquid in tank		External excitation	
Liquid width $(2d)$	2.0m	Excitation amplitude (a)	0.01m
Liquid height (H_L)	1.0m	Excitation frequency (ω)	variable
Liquid density (ρ)	1,000kg/m^3	Relative damping ratio (μ)	0.05

opening width d_B/d of baffle is set by 0.5. Together with the baffle number, the resonance frequency and the peak elevation height show a uniform decrease. Thus, we can obtain the sloshing suppression improvement by increasing the baffle number, and this trend suggests that one can control the fundamental resonance frequency by adjusting the baffle number.

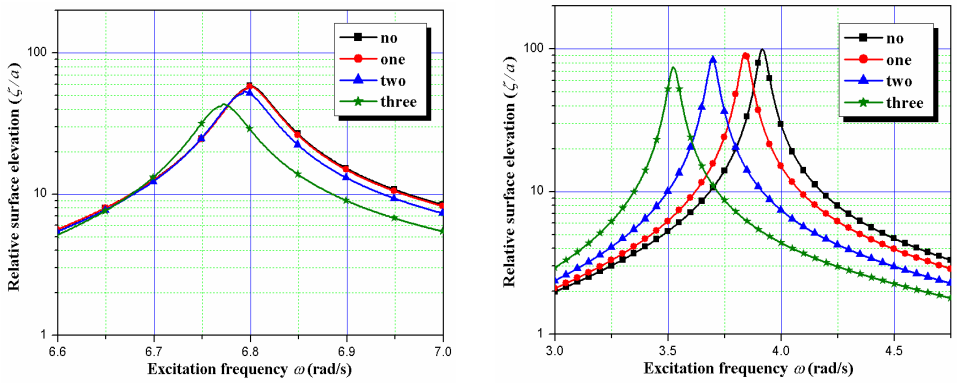

(a) (b)

Figure 3: Frequency response to the baffle number $(d_B/d = 0.5)$: (a) near fundamental resonance frequency; (b) near second resonance frequency.

Fig. 4(a) depicts the parametric variation of the free-surface elevation near the fundamental resonance frequency with respect to the relative baffle height. The peak elevation height and the resonance frequency reduce in proportional to the baf-

fle installation height, and the reduction ratio becomes higher as baffle approaches the liquid free surface. The importance of the baffle height is apparent at the second resonance frequency, as shown in Fig. 4(b), such that the resonance response displays a big difference above and below $H_B/H_L = 0.7$.

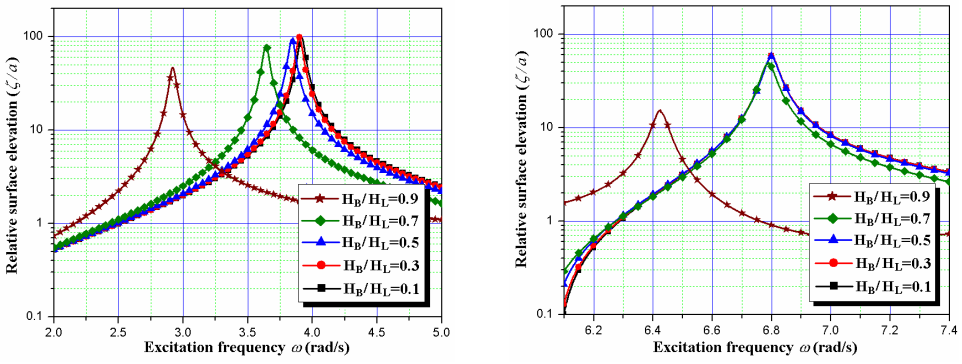

Figure 4: Frequency response to the baffle height (one baffle with $d_B/d = 0.5$): (a) near fundamental resonance frequency, (b) near second resonance frequency.

Conclusion

The resonance sloshing response of liquid contained in 2-D baffled tank subject to the lateral harmonic excitation has been numerically investigated. We confirmed the validity of the artificial damping introduced into the kinematic surface condition to reflect the eminent dissipation effect in the resonant liquid sloshing. As well, the parametric effects of the baffle number and the baffle height have been parametrically examined.

References

1. Cho, J. R. and Lee, S. Y. (2003): "Dynamic analysis of baffled fuel-storage tanks using the ALE finite element method", *International Journal for Numerical Methods in Fluids,* Vol. 41, pp. 185-208.
2. Faltinsen, O. M. (1978): "A numerical nonlinear method of sloshing in tanks with two-dimensional flow", *Journal of Ship Research,* Vol. 22, No. 3, pp. 193-202
3. Cho, J. R., Song, J. M. and Lee, J. K. (2001): "Finite element techniques for the free-vibration and seismic analysis of liquid-storage tanks", *Finite Elements in Analysis and Design,* Vol. 37, pp. 467-483.